Large Scale Simulations for Carbon Nanotubes

Project Representative
Syogo Tejima Research Organization for Information Science & Technology

Authors
Syogo Tejima*1, Satoshi Nakamura*1, Kohji Makino*1, Yutaka Maniwa*3,
Yoshiyuki Miyamoto*4, Yoshikazu Fujisawa*2 and Hisashi Nakamura*1

*1 Research Organization for Information Science & Technology (RIST)
*2 Honda R&D Co., Ltd
*3 Tokyo Metropolitan University
*4 Fundamental and Environmental Research Laboratories, NEC Corporation

CARBON NANOTUBE RESARCH GROUPE
Morinobu Endo, Eiji Osawa, Atushi Oshiyama, Yasumasa Kanada, Susumu Saito,
Riichiro Saito, Hisanori Shinohara, David Tomanek, Tsuneo Hirano, Shigeo Maruyama,
Kazuyuki Watanabe, Takahisa Ohno, Yutaka Maniwa, Yoshikazu Fujisawa,
Yoshiyuki Miyamoto, Hisashi Nakamura

Nano carbon materials as nanotubes (CNTs) and fullerenes in nanotechnology have a lot of potential for industrial applications. On the efforts of developing applications, it has been recognized that computational simulations are powerful and efficient tools to find and create new materials from nano scale. Aiming at realistic simulations for nonmaterial, we have developed a large-scale computation technique utilizing tight binding molecular dynamic method, ab initio density functional theory (DFT), and time-dependent DFT method. We have studied various physical properties of nano-carbon and applications e.g., (1) Growth mechanism of carbon nanotube, (2) Characteristics of Mackay structure, (3) Hole-doped diamond superconductor, (4) Quantum Transport for molecular wire, (5) Irradiation of strong optical field on nano-carbons, (6) One-dimensional magnetic oxygen ordering in CNT, (7) Order-N first principle method for large scale system.

Along these works, we have realized that the Earth Simulator is a very powerful tool for large-scale material simulations.

Keywords: Large scale simulation, TB theory, ab initio theory, DFT, Carbon Nanotube, Fullerenes, GSW, CNT growth, Hydrogen storage, Hole-doped Diamond superconductor

1. INTRODUCTION

Carbon materials have been expected to make a breakthrough in material science and nanotechnology. A lot of potential applications of nanotubes and fullerenes e.g., electronic field emitter and electronic devices have attracted scientific community. In investigating and utilizing their material properties, numerical simulation by means of supercomputer has turned out to be a very efficient tool. A recent development in nanotechnology has required a more efficient supercomputing capable of a large-scale simulation of up to ten thousand atoms. Aiming at large-scale simulations utilizing the Earth Simulator, we have developed computational package based on *ab initio* DFT theory and parameterized tight-binding method. The TB code we have developed is shown to be suitable for the very large systems even though the lack of symmetrical arrangement. The Eliashberg equation linearized with respect to the anomalous Green's function applied to the prediction of high *Tc* superconductivity for a hole-doped diamond. We have carried out some subjects in this work, which are described in the next section. There are three primary objectives with this work: (1) design of innovative nonmaterial with certain desired properties; (2) obtaining fundamental properties in nano-scale matter, and (3) nano-applications. Our purpose is to give the clear explanation of properties and phenomena of nano-scale events and deduce guiding principle to design new materials for applications from nanostructures using super-computers.

2. Physical studies on nano materials

2.1 Growth Mechanism of Carbon nanotube

Controlling growth process of SWCNT in the presence of a metallic catalyst is an essential requirement to provide high

quality CNT for electrical and thermal transport wire in applications. There has been large progress in the experimental mass production of SWCNT. Nevertheless, the growth mechanism of high quality SWCNT is still poorly understood. On the basis of such experimental results, we presented a scenario for an acceptable SWCNT growth process, which are constructed from four stages. In this scenario, the metal cluster plays two important roles in the growth process. The first is to act as a hydrocarbon decomposition catalyst to produce C atoms (stage 1). The second is to act as a solvent for the C atoms (stage 2, 3, 4).

Using a first principle molecular dynamics calculation, we examined a decomposition of Methane molecules by catalysis. The reason we used quantum rather than classical methods is that it is difficult for classical method to consider strong quantum effects of H atoms having small mass. Stage 1: From a simulation at 1100 K, methane molecule is dissociated into C and H atoms on the surface of the catalysis as shown in Fig. 1. The isolated flying H atoms tend to become hydrogen molecules by binding. On the contrary, C atoms tend to remain on the surface of catalyst during the simulation. We speculate that due to the lack of simulation time, we could not observe the diffusion of C atoms entering the catalyst.

After decomposition of hydrocarbon atoms, C atoms for the CNT growth are placed at the surface of the catalyst. According to our assumption, H molecules do not play an important role in growth of SWCNT; therefore we consider a behavior of C atoms only. On the basis of such a reason, we can introduce an empirical classical molecular dynamic simulation to deal with C and Fe atoms except for H atoms.

From the classical molecular dynamics simulations based on empirical potential, we obtained very interesting behavior of C atoms in the presence of Fe cluster composed of 55 atoms. Stage 2: until containing about 25 atoms of C in cluster, C atom remain inside the cluster with diffusion. Stage 3: Over about 25 atoms of C, C atom saturates inside the cluster and precipitate on the surface of Fe cluster. Stage 4: The precipitated carbon atom creates a carbon cloud near the surface. At last, caped carbon structure lifts up from Fe cluster. Such carbon structure is certainly tubular structure not carbon nanotube. The tubular structure possesses sp^3 hybridization and tube hollow are filled with C atoms as shown in Fig. 2.

Simulation results depend on conditions like a hydrocarbon flow constraint, system temperature, and size of Fe cluster. From the detailed research for the effect of these conditions on the SWCNT growth process, we will find the best condition which helps understanding of the growth of CNT.

2.2 Characteristics of the Mackay structure [1]

We have focused on the Mackay structure that consists of only carbon and expects useful characteristics (stable, very rigid, magnetic body, and so on). Three production processes from connecting carbon nanotubes to the Mackay structure were found out by using only sequential GSW rearrangements in last year. However, only small size structure's energy was obtained, because the amount of calculation is very huge. Then, the each energy of larger size structures is calculated newly. Figure 3 shows the energy of each structure. Although there is energy barrier in the production process,

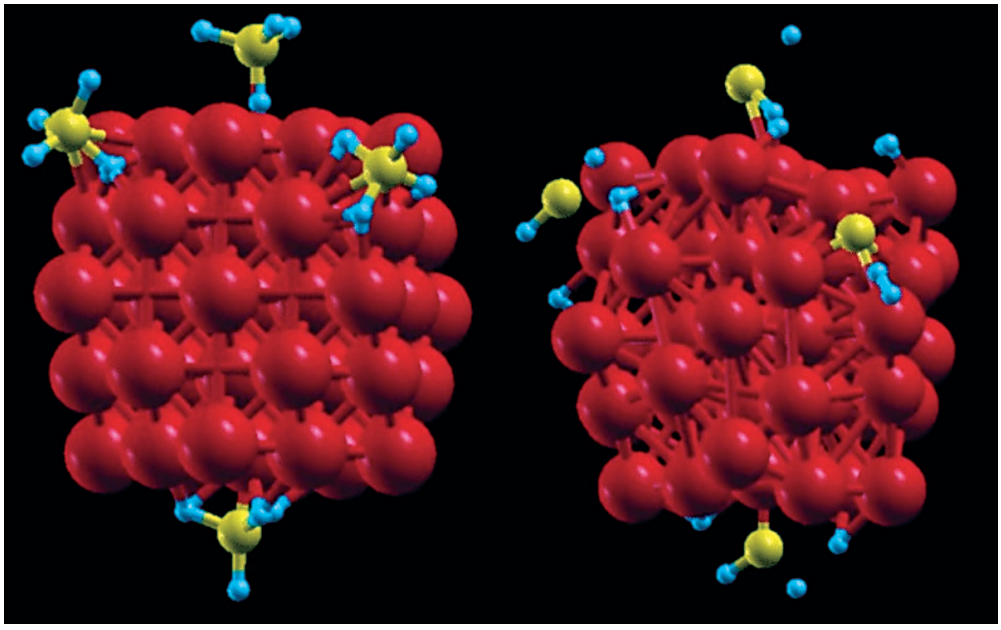

Fig. 1 Fore methane molecules are placed on the Fe cluster of (001) and (111) surface in a initial structure (left figure). After 54ps using first principle MD simulation, methane molecules are decomposed into H and C , and one hydrogen molecule appears (right figure).

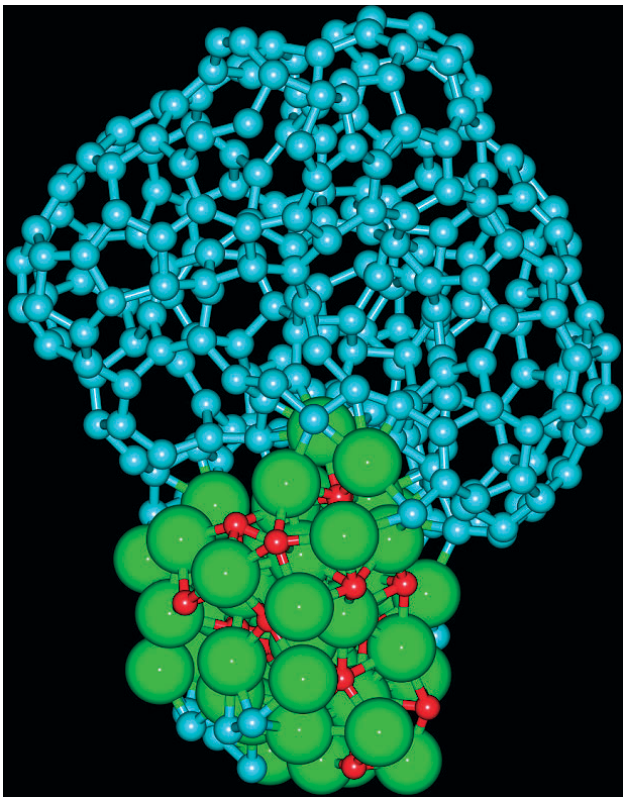

Fig. 2 After 10 ns using an empirical classical simulation, carbon tubular structure is created on the Fe catalyst. Green circle shows Fe atom red isolated carbon atom, blue bonding carbon atom.

the barrier is not so high. These results confirm that there is the possibility of the realization of the Mackay structure.

Furthermore, we clarified that the Mackay structure can be distinguished into two types: zigzag and armchair type. This difference is the direction of six-membered ring (Fig. 4). Zigzag type has been known, but armchair type has not. Some researchers have analyzed smaller zigzag types with computer simulation. In this research, the characteristics of large size and/or armchair type Mackay structure and are examined. However, in order to investigate characteristics

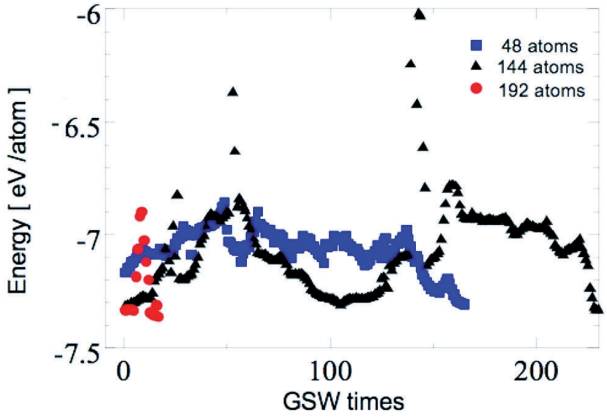

Fig. 3 Energy of each structure.

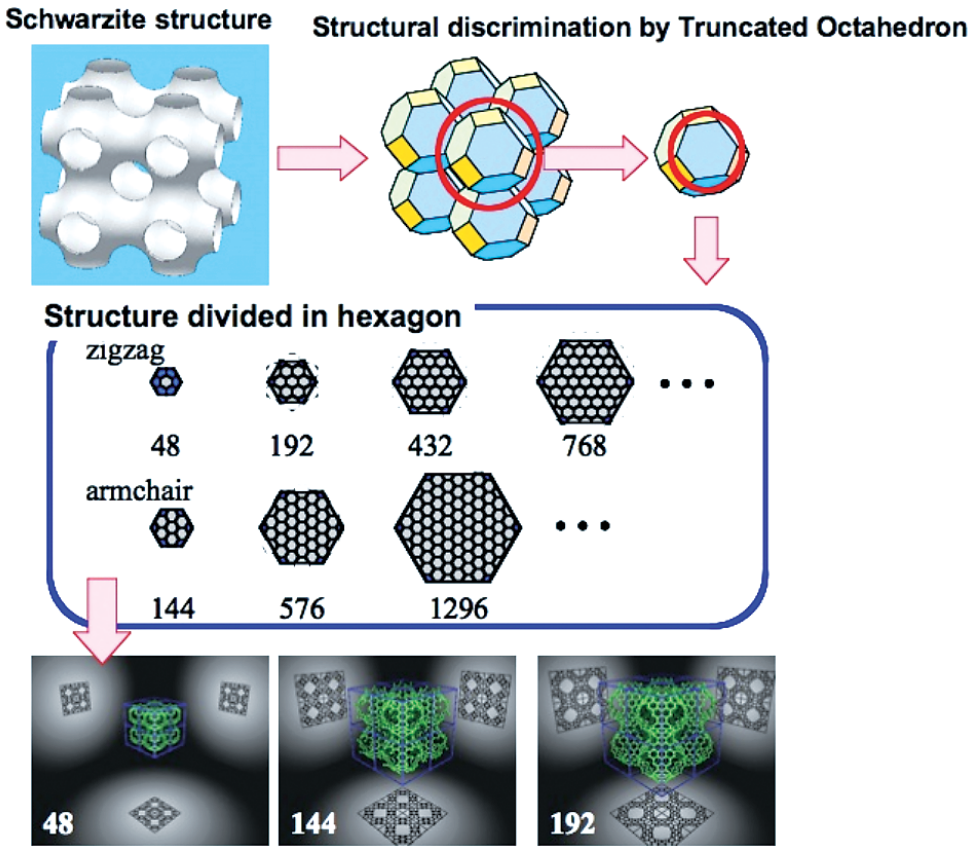

Fig. 4 Zigzag and armchair type of the Mackay structures.

of large size structure, a large scale computer is necessary. Therefore, large structures have not been dealt with. First, bulk modulus is investigated. The results are shown in Fig. 5. The smallest structure is almost as rigid as diamond and is more rigid than large one. Moreover, there was no difference according to the types. Next, it has been guessed that the carbon atoms in the Mackay structure are arranged along the faces of Schwarz's minimal p-surface (Fig. 4:upper-left). However, the carbons are arranged along the faces of truncated octahedron (Fig. 6). The results are useful to analyze the characteristics of the Mackay structure. Finally, the electric is calculated with PWscf code. E-dos of 3 Mackay structures are illustrated in Fig. 7. As a consequence, the Mackay structures have semiconducting property.

2.3 Hole-doped diamond superconductor

We have been evaluating the critical transition temperature (Tc) of hole-doped diamond on the basis of the charge fluctuation mechanism. The result of our calculation last year showed that pure diamond with 0.03 holes per atom was possibly the superconductor with 75 (K). The Tc's observed in experiments, however, are lower than those esti-

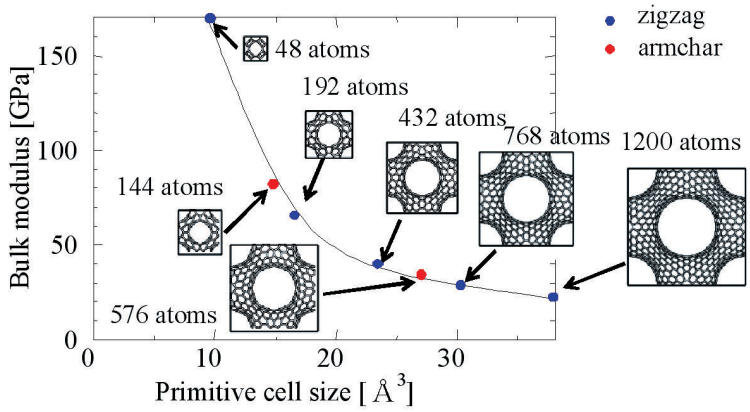

Fig. 5 The relationship between primitive cell size and bulk modulus.

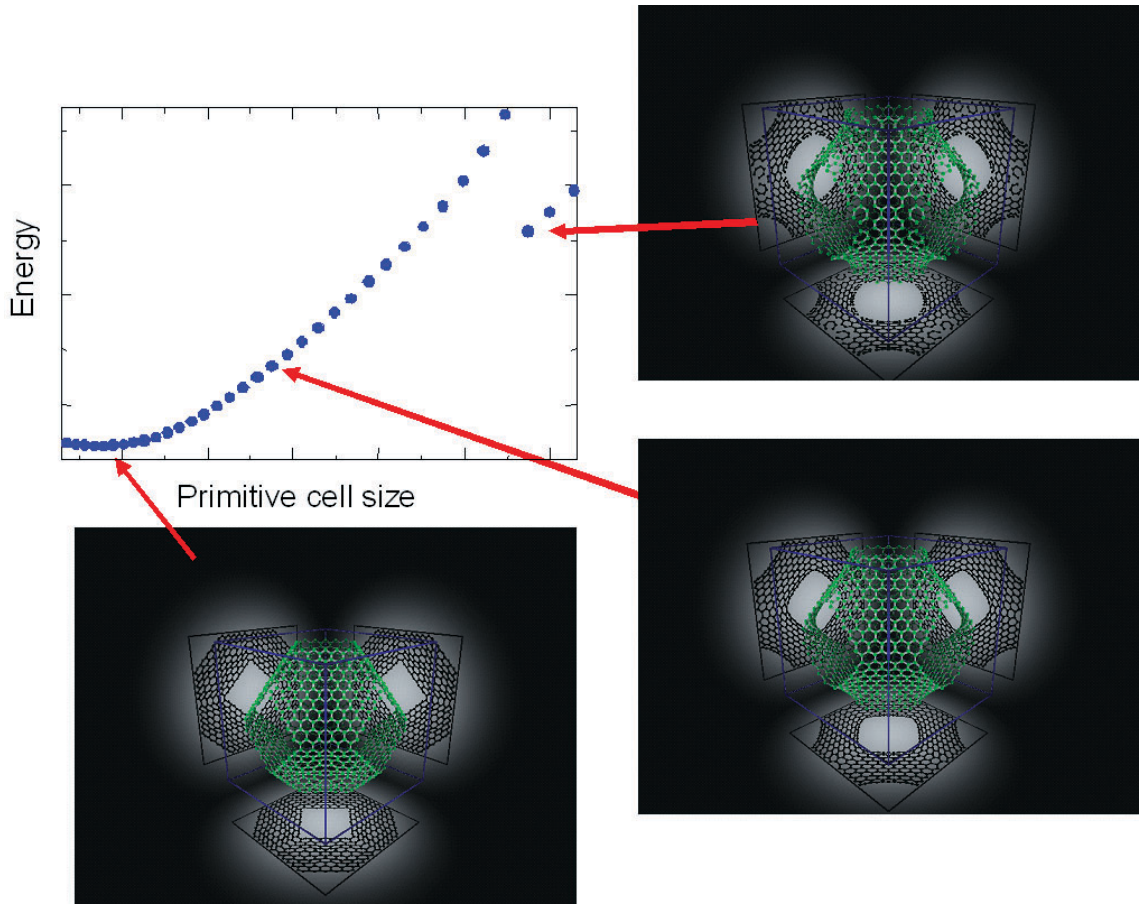

Fig. 6 Stable shape of the Mackay structure.

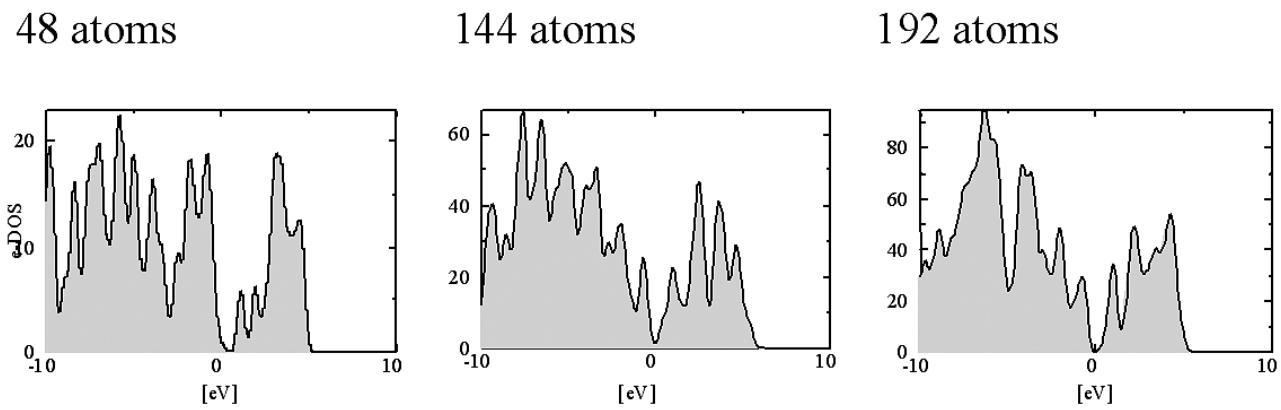

Fig. 7 E-DOS of 48, 144 and 192 atoms of the Mackay structures.

mated by simulation. At the present, the maximum value of Tc is 7 (K). This discrepancy seems to be attributed mainly to the method of incorporating the bare Coulomb interaction within the tight-binding approximation. In the simulation achieved last year, the spatial spread of atomic orbitals has not been taken into account at all.

According to the consideration of this spatial spread, the bare Coulomb interaction V has to have the following two limits:

$$\lim_{|\boldsymbol{R}_{j1}-\boldsymbol{R}_{j2}|\to 0} V_{\varepsilon 1,\eta 1;\varepsilon 2,\eta 2}(\boldsymbol{R}_{j1}-\boldsymbol{R}_{j2}) = U^{\mathrm{at}}_{\varepsilon 1,\eta 1;\varepsilon 2,\eta 2}$$

$$\lim_{|\boldsymbol{R}_{j1}-\boldsymbol{R}_{j2}|\to \infty} V_{\varepsilon 1,\eta 1;\varepsilon 2,\eta 2}(\boldsymbol{R}_{j1}-\boldsymbol{R}_{j2}) = U_{\varepsilon 1,\eta 1;\varepsilon 2,\eta 2}(\boldsymbol{R}_{j1}-\boldsymbol{R}_{j2}),$$

where

$$U_{\varepsilon 1,\eta 1;\varepsilon 2,\eta 2}(\boldsymbol{R}_{j1}-\boldsymbol{R}_{j2}) = \frac{e^2}{4\pi\varepsilon_0}\left[\frac{\delta_{\varepsilon 1\eta 1}\delta_{\varepsilon 2\eta 2}}{|\boldsymbol{R}_{j1}-\boldsymbol{R}_{j2}|} + \frac{\boldsymbol{P}_{L1}-\boldsymbol{P}_{L2}-(\boldsymbol{R}_{j1}-\boldsymbol{R}_{j2})\cdot(\boldsymbol{P}_{L1}-\boldsymbol{P}_{L2})}{|\boldsymbol{R}_{j1}-\boldsymbol{R}_{j2}|^3} - \frac{3\{(\boldsymbol{R}_{j1}-\boldsymbol{R}_{j2})\cdot\boldsymbol{P}_{L1}\}\{(\boldsymbol{R}_{j1}-\boldsymbol{R}_{j2})\cdot\boldsymbol{P}_{L2}\}}{|\boldsymbol{R}_{j1}-\boldsymbol{R}_{j2}|^5}\right],$$

and U^{at} is intra-atomic bare Coulomb interaction. For the sake of simplicity, the value of U^{at} was set at 8 (eV) for the diagonal components and 0 (eV) for the off-diagonal components. As a function that interpolates between these two limits, we have adopted

$$V_{\varepsilon 1,\eta 1;\varepsilon 2,\eta 2}(\boldsymbol{R}_{j1}-\boldsymbol{R}_{j2}) = \frac{U^{\mathrm{at}}_{\varepsilon 1\,\eta 1;\varepsilon 2\,\eta 2}U_{\varepsilon 1\,\eta 1;\varepsilon 2\,\eta 2}(\boldsymbol{R}_{j1}-\boldsymbol{R}_{j2})}{U^{\mathrm{at}}_{\varepsilon 1,\eta 1;\varepsilon 2,\eta 2}+U_{\varepsilon 1,\eta 1;\varepsilon 2,\eta 2}(\boldsymbol{R}_{j1}-\boldsymbol{R}_{j2})}.$$

We show in Fig. 8 the value of Tc's against hole-concentration. The figure represents that for relatively high hole-concentration, Tc's are lower than those simulated last year. In this way, the discrepancy between the simulation and experimental results has been improved.

2.4 Quantum Transport for molecular wire

Application of carbon nanotubes as electronic devices had been expected due to their unique properties. Devices such as random access memory and radio receiver have already been developed up to a considerable stage. In order to fully achieve control on the properties of carbon nanotube-based devices, it is important to perform analyses of the carbon nanotubes of which sizes are the same as those observed in experiments.

To this aim, we have developed a extended tight-binding molecular dynamics method based on conventional tight-binding molecular dynamics method. A conventional tight-binding molecular dynamics method neglects the following

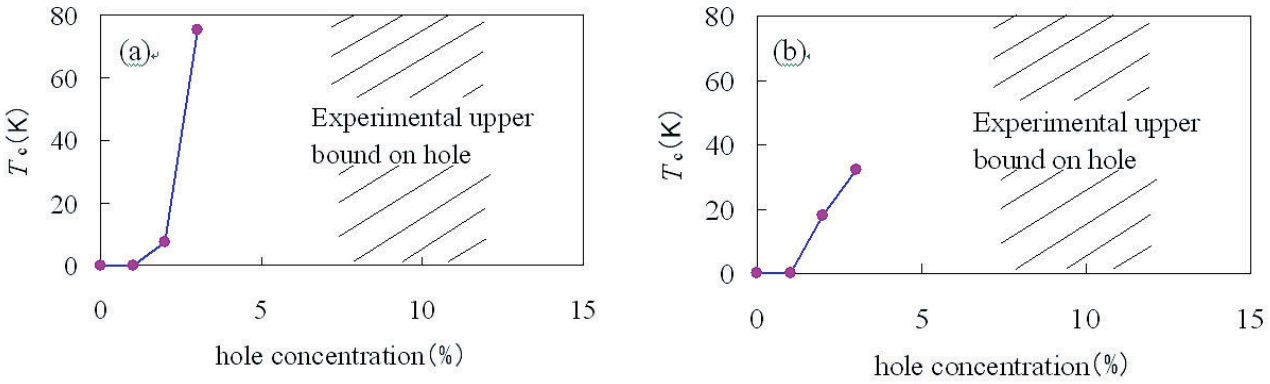

Fig. 8 Tc's against hole-concentration. (a) Result simulated last year. (b) Result simulated this year.

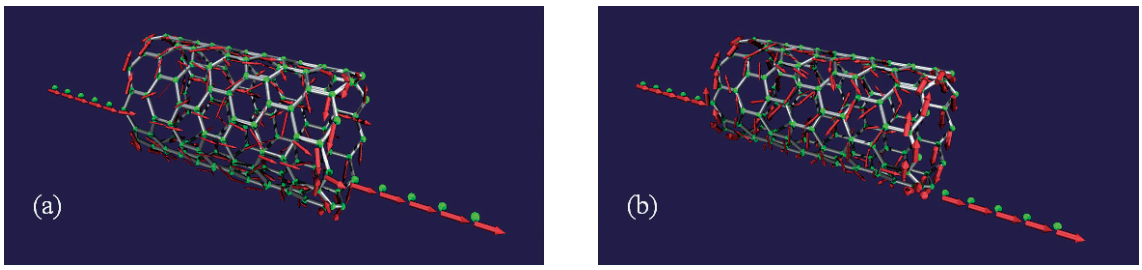

Fig. 9 Electrical current distribution in the nanotube attached to one-dimensional electrodes. The diameter of the arrow indicates the magnitude of the current in log scale. (a) The line connecting two electrode-junctions is parallel to the axis of the nanotube. (b) The line connecting two electrode-junctions is not parallel to the axis of the nanotube.

effects.: A change in long range Coulomb interaction due to a change in the electronic density distribution and polarization within carbon atoms. We have formulated, therefore, a tight-binding molecular dynamics method incorporating these effects. Furthermore, to treat carbon atoms in the electro-magnetic field, this method was combined with the microscopic Maxwell's equations.

As a test calculation, we show in Fig. 9 the electrical current distribution in the nanotube attached to one-dimensional electrodes. A detailed investigation is left for future work.

2.5 Application of time-dependent density functional theory for irradiation of strong optical field on nano-carbons [2]

In the last year, we developed our time-dependent density functional theory (TDDFT) code being available for computing material response under time-varying strong external field. We develop formalisms to compute 'work' done by the external field and confirm that increase of total energy (including kinetic energy of ions) is the same as the work. This means our numerical simulation goes under stable condition.

This year, we apply the code for two subjects. The one is structural change of graphite surface irradiated with pulse laser. Recently, mono-atomic layer of graphene sheet has attracts high attention since mono-layer graphene has been expected to show ballistic transport property, mechanical and thermal robustness. However, the massive production of mono-layer graphene is still challenging and usual processes (scotch tape, CVD, solvent treatment, etc.) suffer from contaminant. We were searching a way to make structural transition of graphite surface into diamond phase by strong laser pulse, but just by accident, we discover a condition of exfoliation of single-layer graphene sheet.

In this calculation, we use periodic boundary condition consisting of 10-layer AB-stacked 2 × 2 unit cell of graphite with vacuum region of 10Å. The optical field by laser pulse was mimicked by fictitious dipole charge layers uniformly expand in parallel direction to graphite layer at the middle of the vacuum region making sawtooth type potential, which is a standard way of investigating the field effect. But this time, the field varies with respect to time as

$$E(t) = E_0 \sin(\omega t) \exp\left(\frac{t - t_0}{\tau}\right)$$

where, w and t respectively correspond to 800 nm of light wavelength and 50 fs of pulse width. The maximum strength of field E0 has been set as 1.6 V/Å as arbitrary test and we found with this condition the surface structure of graphite shows structural change shown in Fig.10 as below.

We expect the current condition will be realized by femtosecond laser technique and also expect other structural change, like graphite-diamond transition, will also be observed by modifying the pulse shape and wavelength of laser shot.

The other application of TDDFT with time-varying external field is penetration of optical field inside semiconducting carbon nanotubes. It is well known that semiconducting nanotubes shows fluorescence depending on their chiralities. The dependence is owing to their unique high density of state of one-dimensionality. Recently, precise experiments can realize optical transition with polarization of optical field perpendicular to tube axis which opposed to previous understanding that nanotubes completely depolarize the optical field in such polarization.

Motivated by the recent experiments, we investigate how depolarization is strong by monitoring induced dielectric field at the center of semiconducting nanotubes under external dielectric field. We have tested two semiconducting nanotubes, (8,0) and (14,0) tubes. In both cases, we found that significant enhancement of field tentatively occurs when frequencies of the applied dielectric field are close to the resonance of excitation energies of these nanotubes. In contrary, when the frequency is out-of-resonance, the dielectric field inside nanotubes is significantly attenuated. Figure 11, shows the current results. From top to bottom, blue lines denote time-evolution of applied field while the red lines denote the allied field plus induced field by nanotubes (called as total field). Note that only the top of Fig.11 shows off-resonance condition. This finding raises further interest for optical excitation of molecules being encapsulated inside

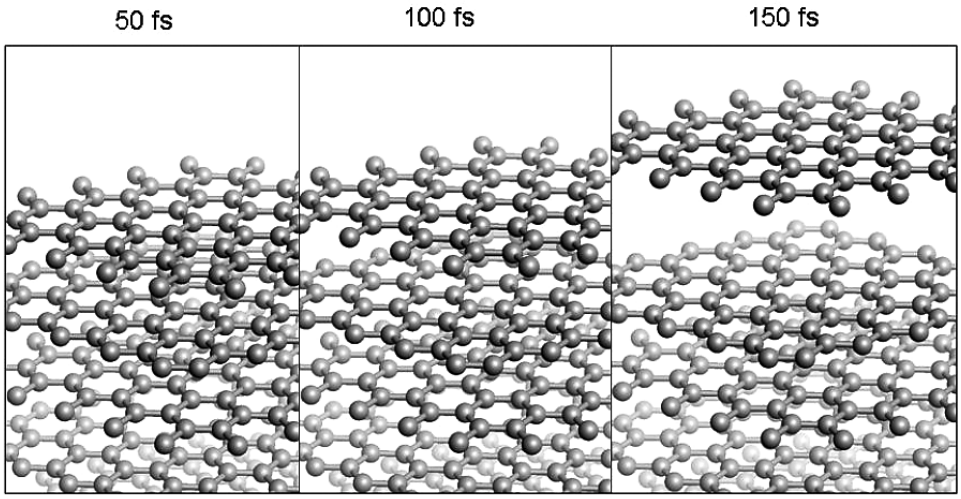

Fig.10 Time evolution of graphite surface after irradiation of laser shot.

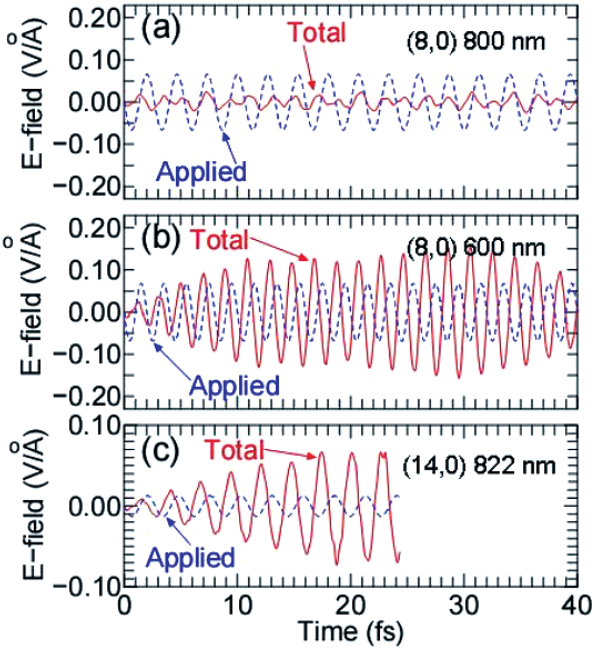

Fig.11 Field enhancement in semiconducting nanotubes. Blue and red lines are time-evolution of applied and total electric field.

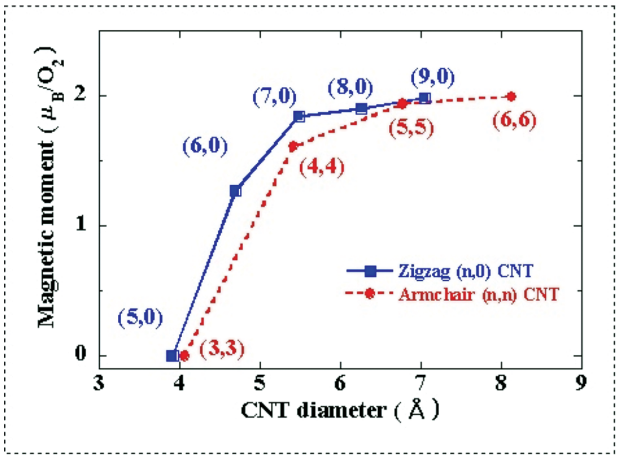

Fig.12 Amplitude of the magnetic moment of oxygen molecule inside (m,0) and (n,n) CNTs.

semiconducting nanotubes. By tuning the chiralty of nanotubes, nanotube excitation energy can be adjusted to that of molecule. If this is the case, we obtained higher quantum efficiency of optical transition because of the enhancement of optical field inside nanotubes.

2.6 One-dimensional magnetic Oxygen ordering in CNT

Oxygen molecule is an interesting functional molecule with spin S = 1. Therefore, it would be possible to develop novel nanoscale magnetic materials by encapsulation of oxygen molecules inside the carbon nanotubes (CNTs). Here, we examined the structures and electronic states of oxygen-encapsulating CNTs using the computer simulation technique. First, classical molecular dynamics calculations clarified that oxygen molecules form one-dimensional to multi-helix structures with the increasing CNT diameter. Then, the first-principal calculations using pwscf code were conducted on the narrow CNTs with one-dimensional array of oxygen molecules. It was suggested that amplitude of the magnetic moment of oxygen molecule decreases with decreasing the CNT diameter below ~7Å as shown in Fig.12. The results will give important suggestion for the low-dimensional magnetic material design.

2.7 Large scale calculation for application using a sophisticated first principle order-N calculation method [3].

We succeeded in structural optimization by a first principle self-consistent calculation for the nano structure which contained about five thousands atoms. By this code the stability of three dimension pyramid structure is obtained shown in Fig. 13. This sample contains about 23,000 atoms. It is understood to be able to optimize stability and the structure to such a hugeness system.

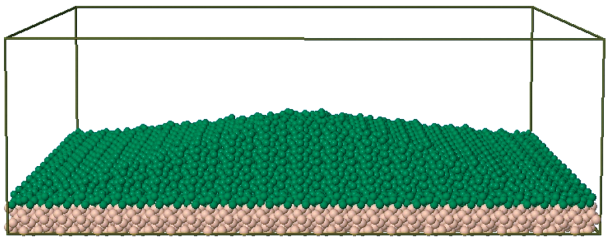

Fig.13 Optimized nano structure in about 23000 atom system.

3. SUMMARY

The large-scale simulations on nonmaterial have been carried out by ab initio density functional method and the parameterized tight-binding calculations. The optimized codes showed that the computation on the Earth Simulator could give an exceptional performance and enables us more chance for large-scale and realistic simulations. Our large scale simulations can provide the nanotechnology industries valuable information on novel nano material properties and on nano electrical designs for application.

References

[1] K. Makino, et al, RIST NEWS No.45.

[2] Y. Miyamoto, and J. Zhang, "Testing the numerical stability of time-dependent density functional simulations using the Suzuki-Trotter formula", Phys Rev B77, 165123 (2008).

[3] T. Miyazaki, et-all, "The energetics of hut-cluster self-assembly in Ge/Si(001) from linear-scaling DFT calculations", J. Phys. Soc. Jpn. in press.

カーボンナノチューブの特性に関する大規模シミュレーション

プロジェクト責任者
手島　正吾　　高度情報科学技術研究機構

著者
手島　正吾*1，中村　　賢*1，牧野　浩二*1，真庭　　豊*3，宮本　良之*4，藤沢　義和*2，中村　　壽*1

*1　高度情報科学技術研究機構
*2　株式会社　本田技術研究所
*3　首都大学東京
*4　NECラボラトリーズ　基礎研究所CNT応用研究センター

1. 研究目的

優れた物性が予想されナノテクの基本材であるナノ炭素類（カーボンナノチューブ（CNT）、フラーレン、グラフェン）の電子・機械特性を従来不可能だった大規模シミュレーションにより推定し、科学技術及び産業界に提供すると共に、応用として特性の優れた新構造を発見し、基本材の拡充に寄与する目的で実施された。

2. 成果

H14年度、地球シミュレータを利用した大規模シミュレーションの有効性を世界に先駆けて実証した。また、H15・H16・H17・H18・H19 年度は、我が国のナノチューブ研究で当面する課題解決に向けた応用シミュレーションを実施した。本年度さらに、応用シミュレーションを推進し得られた結果を以下に示す。(1) 良質のカーボンナノチューブを得るための気相でのカーボンナノチューブ成長過程について、第一原理計算により電子論の立場から供給炭化水素の触媒金属原子鉄による炭素・水素分解過程を確認し、また古典分子動力学計算により分解で生じた炭素が触媒内部に拡散、飽和を経て触媒表面から析出しナノチューブ生成が開始される過程を確認した。(2) 新物質創世のためのマッカイ型炭素構造材については、大きさやタイプの異なるマッカイ構造を系統的にシミュレーションし、カーボンナノチューブから変形していく際の結合エネルギーから実現の可能性を示す結果を得、さらにマッカイ構造の機械特性、電子構造特性を明らかにした。(3) 高温超伝導体の研究からは、ボロンをホールとして含有させたダイヤモンド複合構造（薄膜構造）の高温超伝導体に対して、電子間のクーロン相互作用に内挿式を用いて改良した結果、前年度よりも高精度のT_cを得ることに成功した。(4) 分子を流れる電子の量子伝導を解析するために、電荷ゆらぎ、分極および電磁場の効果をパイエルス位相として取り入れた強結合分子動力学法を構築した。膨大な計算量を必要とする2電子積分を行わず分極の効果までを考慮したクーロン相互作用で近似することによって計算量を大幅に軽減し、大規模な分子動力学計算を可能にした。(5) ナノスケール加工にかかわるシミュレーションでは、パルス発生の効果を入れたTDDFT（時間依存密度汎関数理論）を利用した分子動力学計算にて、グラファイトのバルクにパルス電場を与え、グラファイトの最表面の1層のグラフェンがはがれていく過程が得られ、界面活性剤に変わる技術を提案した。光電場の半導体ナノチューブのシミュレーションに対し、印加電場の振動周期とナノチューブ励起エネルギーの共鳴増大効果により壁の局率が負になるナノチューブ内部ですらも、電界増大を見ることが可能となった。(6) 新機能材料として、磁性を有する機能的分子である酸素をカーボンナノチューブ円筒空洞内閉じ込めることによる酸素磁性体の創製を試みた結果、第一原理電子状態計算により、CNT内部に酸素分子が1次元的に配列しCNT直径が小さくなると酸素分子の磁性が消失する傾向を示した。(7) オーダーN法第一原理計算ではモデル開発が完了し、ナノ構造物質に関しては約5千原子を含む系に対してセルフコンシステント計算による構造最適化、生体系に関しては、多数の水分子を含むDNAの系や膜タンパク質に対して構造最適化などを実現することに成功した。

キーワード：大規模シミュレーション, タイトバインディング理論, 時間依存密度汎関数法, オーダーN法,
カーボンナノチューブ, マッカイ構造, グラファイト加工技術, ナノチューブ共鳴電場, 1次元酸素磁性体,
ホールドープダイヤモンド高温超伝導体, 量子伝導